Factors influencing the island-mass effect of the Galápagos Archipelago

Daniel M. Palacios

College of Oceanic and Atmospheric Sciences, Oregon State University, Corvallis, Oregon, USA

Received 5 September 2002; accepted 4 October 2002; published 13 December 2002.

[1] Enhanced phytoplankton biomass in the wake of the Galápagos Islands is thought to result from an island-mass effect (IME) fueled by upwelling of the Equatorial Undercurrent (EUC) and by natural iron enrichment from the island platform. Annual means of five variables describing the thermocline, the pycnocline, and the availability of nitrate at the surface were derived from the World Ocean Atlas 1998 (WOA98). The first principal component of these variables explained 55.8% of the variance, corroborating that the Galápagos IME is associated with features of the EUC, mainly a shallow thermocline/pycnocline and its vertical spreading in the vicinity of the Galápagos. Regression analysis of SeaWiFS-derived chlorophyll-*a* (chl) on the WOA98 variables indicated that the depth of the thermocline and nitrate availability explain 91.9% of the chl variance. A secondary IME of enhanced chl levels associated with the wind-sheltered area north of Isabela Island was evident in the residual variability. *INDEX TERMS:* 4231 Oceanography: General: Equatorial oceanography; 4279 Oceanography: General: Upwelling and convergences; 4536 Oceanography: Physical: Hydrography; 4572 Oceanography: Physical: Upper ocean processes; 4855 Oceanography: Biological and Chemical: Plankton. **Citation:** Palacios, D. M., Factors influencing the island-mass effect of the Galápagos Archipelago, *Geophys. Res. Lett.*, *29*(23), 2134, doi:10.1029/2002GL016232, 2002.

1. Introduction

[2] Biological enhancement in the vicinity of oceanic islands is a well-documented phenomenon. This "island-mass effect" (after *Doty and Oguri* [1956]) can contribute to the productivity and potential fisheries near islands [*Heywood et al.*, 1990; *Signorini et al.*, 1999], and may be significant to the global CO_2 budget [*Heywood et al.*, 1996]. Several non-exclusive, causative mechanisms have been described: lee eddies formed by flow disturbance or by Ekman pumping [e.g., *Coutis and Middleton*, 1999; *Barton et al.*, 2000]; nutrient input from island runoff [e.g., *Bucciarelli et al.*, 2001; *Perissinotto et al.*, 2000]; drainage from an internal lagoon [*Sander*, 1981]; and contributions from benthic processes [*Doty and Oguri*, 1956; *Dandonneau and Charpy*, 1985].

[3] The topographically forced upwelling of the eastward-flowing Equatorial Undercurrent (EUC) as it collides with the western side of the Galápagos Archipelago (0.5°S, 90.5°W) [*Houvenaghel*, 1978] has been linked to enhanced production of phytoplankton [*Jimenez*, 1981; *Feldman*, 1986; *Chavez*, 1989] and zooplankton [*Arcos*, 1981]. Once at the surface, the upwelled waters are carried westward by the South Equatorial Current (SEC), the prevailing surface flow in the region, creating a productive habitat that sometimes extends offshore for several hundred kilometers [*Feldman*, 1986]. Phytoplankton blooming in the wake of the Galápagos contrasts with the high-nutrient, low-chlorophyll (HNLC) conditions that persist throughout the rest of the eastern and central equatorial Pacific. It has been recently shown that while EUC upwelling is responsible for the high levels of macronutrients in the area of enhancement, input of high levels of iron derived from the island platform is necessary to support the observed bloom [*Gordon et al.*, 1998; *Lindley and Barber*, 1998].

[4] The Galápagos are located in a hydrographically complex region due to their proximity to the Equatorial Front (located between 1°N and 2°N at the Galápagos). South of the front, equatorial upwelling brings cool and salty water to the surface, while north of the front warm, low-salinity, and stratified waters result from rainfall in the intertropical convergence zone, particularly in the Gulf of Panamá [*Fiedler*, 1992]. The purpose of this paper is to identify the oceanographic conditions that are conducive to the island-mass effect of the Galápagos Archipelago. Climatological water-column data are used to explain phytoplankton distributions, as measured by long-term ocean color observations from NASA's Sea-viewing Wide Field-of-view Sensor (SeaWiFS).

2. Methods

[5] Annual climatologies of water-column properties describing the thermocline, the pycnocline, and the availability of nitrate for primary production were derived from the on-line version of the World Ocean Atlas 1998 (WOA98) at one-degree resolution [*Conkright et al.*, 1998]. At each grid cell, 1-m vertical resolution profiles of temperature, salinity, and nitrate were obtained from the standard depth levels by cubic spline interpolation. The variables derived were: depth of the thermocline (i.e., the depth of the 20°C isotherm, or Z20); thermocline strength (i.e., the vertical distance between the 20°C and 15°C isotherms, or ZTD); maximum Brunt-Väisälä frequency (i.e., the maximum resistance to turbulent mixing in the pycnocline, or MBVF), also known as maximum buoyancy frequency; depth of the MBVF (ZMBVF), also called the depth of the pycnocline; and nitrate concentration at the surface (NO_3). The four physical variables (Z20, ZTD, MBVF and ZMBVF) are necessary to describe the water column because of the effect of the very low-salinity surface layer originating in the Panamá Bight, which results in some uncoupling between

0094-8276/02/2002GL016232$05.00

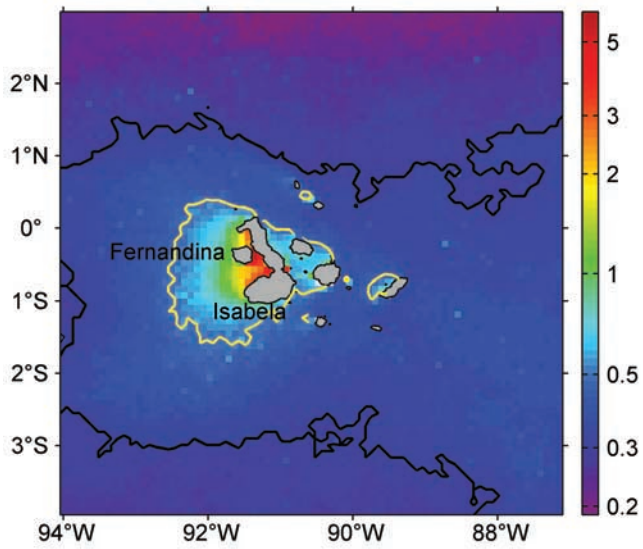

Figure 1. Cumulative average of SeaWiFS-derived chlorophyll-*a* (chl) for the 4.8-yr period 1 September 1997–30 June 2002. Thick black and yellow lines indicate the 0.3 and 0.5 mg m^{-3} contours, respectively. Thin black lines are island coastlines.

thermocline and pycnocline strength (i.e., a weak thermocline is associated with high MBVF).

[6] A cumulative average of satellite-derived chlorophyll-*a* (chl) for the 4.8-yr period 1 September 1997–30 June 2002 at 9-km resolution (Figure 1) was obtained from the SeaWiFS Project (distributed as a Level-3 Standard Mapped Image product, reprocessing No. 4, July 2002). The resolution of this product was lowered by averaging pixels to obtain a data set at one-degree resolution, compatible with the WOA98 data.

[7] A principal component analysis (PCA) was performed on the WOA98-derived water-column variables to rank their relative importance and to describe the dominant patterns of spatial variability in the study area. Multiple linear regression analysis of chl on the WOA98 variables was performed using sequential variable selection procedures to identify the best predictors of chlorophyll abundance.

3. Results

[8] The 4.8-yr chl average (Figure 1) indicates that values are above 0.3 mg m^{-3} in an equatorial band between about 3°S and 1°N, while they are lowest north of 2°N, in the oligotrophic waters north of the Equatorial Front. There are areas of elevated chl (>0.5 mg m^{-3}) associated with most of the major islands. This is most pronounced on the west side of Isabela and Fernandina islands, where the area of enhancement (as defined by the 0.5 mg m^{-3} contour) extends westward for about 120 km and covers about 25,000 km^2. Chl reaches a maximum mean value of 6.2 mg m^{-3} at the southern mouth of Canal de Bolívar, the narrow channel separating Isabela and Fernandina.

[9] Component loadings from the PCA are presented in Table 1 for the first two principal components (PC), which explain 95.5% of the variability in the data sets. The first PC (55.8%) is characterized by a shallow (deep) thermocline (Z20) and pycnocline (ZMBVF), a weak (strong) thermocline (ZTD), and low (high) pycnocline stability (MBVF), leading to high (low) surface nitrate concentrations (NO_3). The second PC (39.7%) contrasts high (low) pycnocline stability and a weak (strong) thermocline with a shallow (deep) pycnocline and low (high) nitrate concentrations. Depth of the thermocline does not contribute to this component (loading = −0.03). Spatially, the site scores depict an equatorial pattern for the first PC (Figure 2a) and a NE-SW pattern for the second PC (Figure 2b).

[10] Correlations between chl and the site scores from the PCA are r = 0.93 and r = 0.035 for the first and second PCs, respectively. Sequential variable selection in the regression analysis of chl on the original WOA98 variables consistently yielded the following model (R^2 = 0.919):

$$\log(chl) = -0.309 - 0.009\ Z20 + 0.115\ NO_3 - 0.019(NO_3)^2 + 0.001(NO_3)^3$$

4. Discussion

[11] From the perspective of long-term ocean color observations from SeaWiFS, the Galápagos IME can be described as a "plume" of elevated chl levels on the west side of Isabela and Fernandina islands that covers an area of about 25,000 km^2. While this area has long been identified as the primary upwelling site of the EUC [*Houvenaghel*, 1978], upwelling alone cannot explain the plume since nitrate levels in surface waters are already adequate to support phytoplankton production in this HNLC region. *Gordon et al.* [1998] showed that upwelled waters become significantly enriched with iron by contact with the island platform, particularly at the Canal de Bolívar, where dissolved iron concentrations of up to 3 nM were measured [*Martin et al.*, 1994]. *Lindley and Barber* [1998] provided evidence that this iron input supports nitrate uptake and elevated primary production in the plume. Although the specific source of island-derived iron has not been identified, resuspension of iron-rich sediment caused by interaction of flow with topography and tidal mixing, particularly in the Canal de Bolívar and in the adjacent bays to the north and south, has been suggested [*Steger et al.*, 1998]. Hydrothermal fluxes from the interior of western Galápagos volcanoes could also be an important source [cf. *Signorini et al.*, 1999].

[12] The westward extent of the plume of about 120 km in the SeaWiFS average compares favorably with the scale length for dissolved iron transport of 103 km estimated by *Bucciarelli et al.* [2001] based on the iron measurements of *Gordon et al.* [1998]. Outside the plume, chl values ≥0.3 mg m^{-3} in an equatorial band between 3°S and 1°N (Figure 1) are explained in terms of wind-driven equatorial upwelling. The EUC has a relatively iron-rich core (0.35 nM at 200 m, 140°W), and the vertical advection of these waters

Table 1. Loadings (Eigenvectors) for the First Two Principal Components (PC) of the WOA98 Variables

	PC 1	PC 2
Z20	−0.59	−0.03
ZTD	0.41	0.49
MBVF	−0.34	0.57
ZMBVF	−0.50	−0.34
NO_3	0.34	−0.57

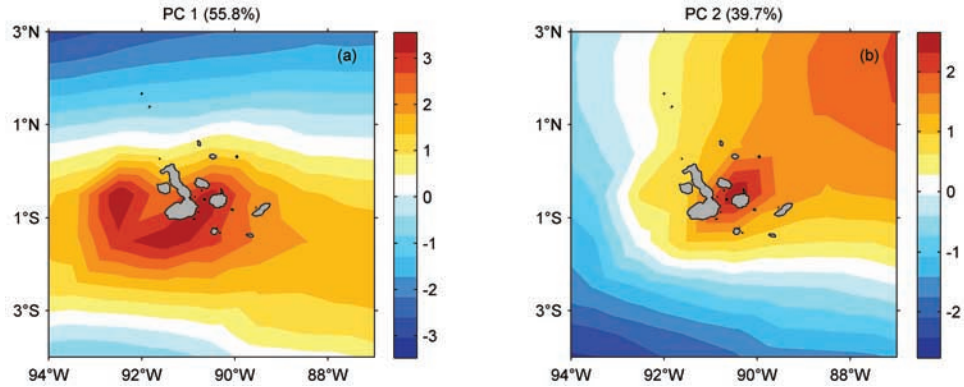

Figure 2. Site scores and explained variance for the first (a) and second (b) principal components of the WOA98 variables.

supports phytoplankton growth throughout the equatorial Pacific [*Gordon et al.*, 1997].

[13] The site scores from the PCA (Figure 2) can be interpreted based on the loadings of the first two principal components (Table 1). The equatorial pattern of the first PC represents a shallow, weak thermocline and pycnocline associated with the EUC (Figure 2a). The highest site scores are associated with the islands and represent the vertical spreading of the thermocline and the weakening of stratification as the EUC encounters the Galápagos. The second PC illustrates a regional NE-SW gradient in pycnocline stratification and shoaling independent of temperature, due to rainfall in the Panamá Bight (Figure 2b). As a result, the distribution of nitrate in surface waters of the study area is closely associated with this stratification regime, as evidenced by the strong inverse relationship with maximum buoyancy frequency ($r = -0.94$, Figure 3a). However, nitrate concentrations also have a somewhat weaker inverse relationship with the depth of the thermocline ($r = -0.52$, not shown). These correlations are consistent with the nitrate loadings onto the second and first PCs, respectively (Table 1).

[14] Correlations between chl and the site scores only support the existence of a relationship for the first PC, which depicts features of the EUC. This suggests that the contributions of the variables to this PC (Table 1) are important for the Galápagos IME. However, while the contribution of nitrate to the first PC is relatively small (loading = 0.34), there is a clear non-linear relationship between chl and nitrate (Figure 3b). This is because the chl-NO_3 relationship adeptly describes the complex response of phytoplankton populations to nitrate and iron availability throughout surface waters of the study area, not only in the plume region. Chlorophyll concentrations are lowest at nitrate concentrations below about 2 μM, representing the oligotrophic conditions north of the Equatorial Front (nitrate is limiting). The high chl values found at intermediate nitrate concentrations (2–6 μM) represent two processes. The first one is equatorial upwelling, which brings both nitrate and EUC iron to the surface and results in enhanced phytoplankton populations and some nitrate removal along the equator [*Gordon et al.*, 1997]. The second one is the phytoplankton bloom in the plume associated with the topographic upwelling of the EUC and the island-derived iron enrichment (i.e., the Galápagos IME), also resulting in

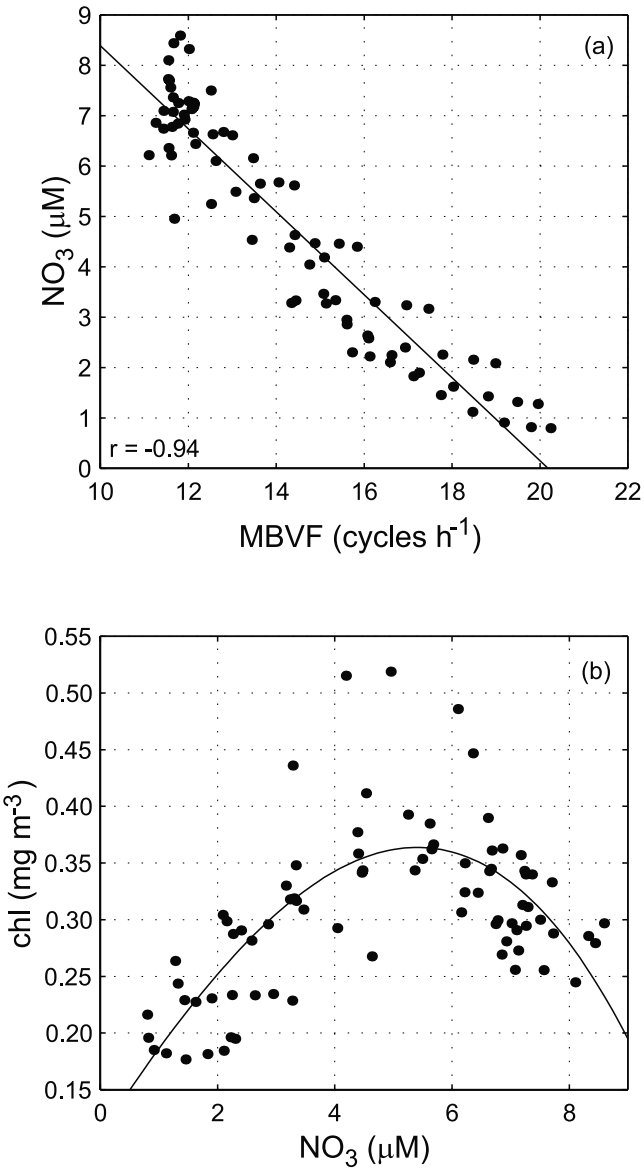

Figure 3. Scatterplots of MBVF *vs*. NO_3 (a) and NO_3 *vs*. log(chl) (b). Least-squares fits are shown.

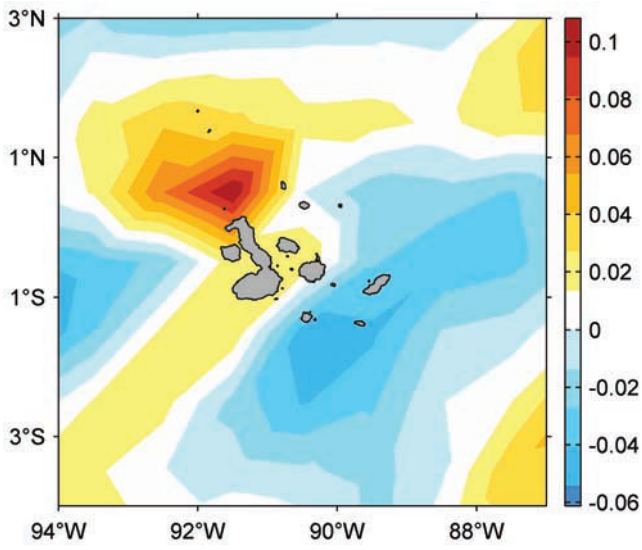

Figure 4. Residual or unexplained chl (in mg m^{-3}) from the multiple linear regression of log(chl) on Z20 and NO_3 (with a third-order polynomial).

nitrate uptake. Finally, the decrease in chl levels at high nitrate concentrations (NO_3 > 6 μM) corresponds to the transition to HNLC conditions, mainly south of the equator, where excess nitrate is not removed due to iron limitation.

[15] Once the curvature in the chl-NO_3 relationship is accounted for by including a third-order polynomial for nitrate, a multiple linear regression model that includes depth of the thermocline and surface nitrate (the two variables with highest loadings in the first two PCs) appears to most adequately explain chl distributions throughout the study area. It should be noted, however, that if a climatological iron data set were available, its inclusion in the regression along with an interaction term with nitrate (NO_3:Fe) would probably account for the observed curvature without a need for the polynomial terms.

[16] While the regression model explained a large fraction (91.9%) of the chl variance, the residual variability contained coherent spatial structures, including an area centered on the north side of Isabela Island with chl levels up to 0.11 mg m^{-3} above the fitted values (Figure 4). This area lies in the lee of Volcano Wolf, the highest elevation in the Galápagos at 1,710 m [*Mouginis-Mark et al.*, 1996]. Given that southeast trade winds prevail in the region for most of the year, I suggest that the observed pattern is created by local Ekman pumping (and iron upwelling from beneath the pycnocline) driven by orographically modified wind stress, as has been observed for other mountainous islands in strong wind regimes [e.g., *Barton et al.*, 2000]. This pattern represents a secondary wind-induced IME. Although the enhancement appears to be comparatively small, this lee region could be an important area of retention and recruitment for zooplankton and larval fish in Galápagos waters.

[17] **Acknowledgments.** The author would like to thank the SeaWiFS Project (Code 970.2) and the Distributed Active Archive Center (Code 902) at the Goddard Space Flight Center, Greenbelt, MD 20771, for the production and distribution of the ocean color data, respectively. The WOA98 data sets were obtained on line from NOAA's National Oceanographic Data Center at ftp://ftp.nodc.noaa.gov/pub/WOA98/. Funding for this study was provided by the Endowed Marine Mammal Program at Oregon State University. Comments from P. T. Strub, C. B. Miller, and two anonymous reviewers greatly improved the clarity of the manuscript.

References

Arcos, F., A dense patch of *Acartia levequei* (Copepoda, Calanoida) in upwelled Equatorial Undercurrent water around the Galapagos Islands, in *Coastal Upwelling*, edited by F. A. Richards, pp. 427–432, Estuarine Sciences 1, American Geophysical Union, Washington, D.C., 1981.

Barton, E. D., G. Basterretxea, P. Flament, E. G. Mitchelson-Jacob, B. Jones, J. Arístegui, and F. Herrera, Lee region of Gran Canaria, *J. Geophys. Res.*, *105*, 17,173–17,193, 2000.

Bucciarelli, E., S. Blain, and P. Tréguer, Iron and manganese in the wake of the Kerguelen Islands (Southern Ocean), *Mar. Chem.*, *73*, 21–36, 2001.

Chavez, F. P., Size distribution of phytoplankton in the central and eastern tropical Pacific, *Global Biogeochemic. Cycles*, *3*, 27–35, 1989.

Conkright, M., S. Levitus, T. O'Brien, T. Boyer, J. Antonov, and C. Stephens, World Ocean Atlas 1998 CD-ROM Data Set Documentation, *Tech. Rep. 15*, NODC Internal Report, Silver Spring, MD, 16 pp., 1998.

Coutis, P. F., and J. H. Middleton, Flow-topography interaction in the vicinity of an isolated, deep ocean island, *Deep-Sea Res. I*, *46*, 1633–1652, 1999.

Dandonneau, Y., and L. Charpy, An empirical approach to the island mass effect in the south tropical Pacific based on sea surface chlorophyll concentrations, *Deep-Sea Res.*, *32*, 707–721, 1985.

Doty, M. S., and M. Oguri, The island mass effect, *J. Cons. int. Explor. Mer*, *22*, 33–37, 1956.

Feldman, G. C., Patterns of phytoplankton production around the Galápagos Islands, in *Tidal mixing and plankton dynamics*, edited by M. J. Bowman, C. M. Yentsch, and W. T. Peterson, pp. 77–106, Lecture Notes on Coastal and Estuarine Studies 17, Springer-Verlag, Berlin, 1986.

Fiedler, P. C., Seasonal climatologies and variability of eastern tropical Pacific surface waters, *NOAA Tech. Rep. NMFS 109*, 1–65, 1992.

Gordon, R. M., K. H. Coale, and K. S. Johnson, Iron distributions in the equatorial Pacific: implications for new production, *Limnol. Oceanogr.*, *42*, 419–431, 1997.

Gordon, R. M., K. S. Johnson, and K. H. Coale, The behaviour of iron and other trace elements during the IronEx-I and PlumEx experiments in the equatorial Pacific, *Deep-Sea Res. II*, *45*, 995–1041, 1998.

Heywood, K. J., E. D. Barton, and J. H. Simpson, The effects of flow disturbance by an oceanic island, *J. Mar. Res.*, *48*, 55–73, 1990.

Heywood, K. J., D. P. Stevens, and G. R. Bigg, Eddy formation behind the tropical island of Aldabra, *Deep-Sea Res. I*, *43*, 555–578, 1996.

Houvenaghel, G. T., Oceanographic conditions in the Galápagos Archipelago and their relationships with life on the islands, in Upwelling ecosystems, edited by R. Boje and M. Tomczak, pp. 181–200, Springer-Verlag, Berlin, 1978.

Jimenez, R., Composition and distribution of phytoplankton in the upwelling system of the Galapagos Islands, in *Coastal Upwelling*, edited by F. A. Richards, pp. 327–338, Estuarine Sciences 1, American Geophysical Union, Washington, D. C., 1981.

Lindley, S. T., and R. T. Barber, Phytoplankton response to natural and experimental iron addition, *Deep-Sea Res. II*, *45*, 1135–1150, 1998.

Martin, J. H., et al., Testing the iron hypothesis in ecosystems of the equatorial Pacific Ocean, *Nature*, *371*, 123–129, 1994.

Mouginis-Mark, P. J., S. K. Rowland, and H. Garbeil, Slopes of western Galapagos volcanoes from airborne interferometric radar, *Geophys. Res. Lett.*, *23*, 3767–3770, 1996.

Perissinotto, R., J. R. E. Lutjeharms, and R. C. van Ballegooyen, Biological-physical interactions and pelagic productivity at the Prince Edward Islands, Southern Ocean, *J. Mar. Sys.*, *24*, 327–341, 2000.

Sander, F., A preliminary assessment of the main causative mechanisms of the "Island Mass Effect" of Barbados, *Mar. Bio.*, *64*, 199–205, 1981.

Signorini, S. R., C. R. McClain, and Y. Dandonneau, Mixing and phytoplankton bloom in the wake of the Marquesas Islands, *Geophys. Res. Lett.*, *26*, 3121–3124, 1999.

Steger, J. M., C. A. Collins, and P. C. Chu, Circulation in the Archipiélago de Colón (Galapagos Islands), November, 1993, *Deep-Sea Res. II*, *45*, 1093–1114, 1998.

D. M. Palacios, College of Oceanic and Atmospheric Sciences, Oregon State University, 104 Oceanography Administration Building, Corvallis, OR 97331-5503, USA. (dpalacio@coas.oregonstate.edu)